NONDESTRUCTIVE CHARACTERIZATIONS OF ALKALI ACTIVATED FLY ASH AND/OR SLAG CONCRETE

Arkamitra Kar
(Graduate Student, MSCE, EIT) West Virginia University, USA
Udaya B. Halabe
(Professor, Civil and Environmental Engineering, PhD, P.E.)
West Virginia University, USA
Indrajit Ray
(Visiting Faculty in Civil Engineering, PhD)
Purdue University Calumet, USA
Avinash Unnikrishnan
(Assistant Professor, Civil and Environmental Engineering, PhD)
West Virginia University, USA

Abstract

In recent years, the alkali activated material (AAM) concrete is emerging as a sustainable and green alternative to traditional portland cement (PC) concrete. In order to widen its applications, more information on correlations among its mechanical and physical properties is required. To address the issue this paper studies the relationships between compressive strength, dynamic modulus of elasticity, and ultrasonic pulse velocity of various AAM concrete mixtures with fly ash and/or slag as precursors cured at different temperatures at both unstressed and stressed conditions. The results show that effective relationships can be established to predict compressive strength and modulus of elasticity from the ultrasonic pulse velocity with reasonable accuracy for wide range of AAM concrete mixes.

Keywords: Alkali activated material concrete, Fly ash, Nondestructive characterizations, Nondestructive testing, Slag

1. Introduction

Portland cement (PC) concrete industry contributes at least 5 – 8% of the global carbon dioxide emissions (Provis and van Deventer, 2009). The decomposition of limestone during the manufacture of cement emits substantial amount of CO_2 and reduces the nature's resource of limestone.

Moreover, the rapid development of infrastructure in various countries all over the world has resulted in the shortage of cement at some places, thereby hampering sustainable development. Hence, there is a need to develop an alternative material, which will not only reduce the demand for PC, but also decrease the CO_2 emissions while possessing mechanical and structural properties comparable to PC. A possible solution to this problem could be the use of alkali activated materials (AAM) or inorganic polymers, which can be produced by reaction of a precursor (fly ash or slag) and an activating solution (alkaline sodium silicate solution and sodium hydroxide mixture). In order to test the suitability of these materials in field applications, it is imperative to evaluate their characteristics in-service. Inorganic polymers, more commonly referred to as ‘‘geopolymers’’, are alumino-silicate materials which exhibit excellent physical and chemical properties. Geopolymers have a diverse range of potential applications, including precast structures and non-structural elements, concrete pavements and products, containment and immobilization of toxic, hazardous and radioactive wastes, advanced structural tooling and refractory ceramics, and fire resistant composites used in buildings, aeroplanes, shipbuilding, racing cars, and the nuclear power industry. In 1979, Professor Davidovits of France produced binders by mixing alkalis with burnt mixture of kaolinite, limestone and dolomite; he coined the term “geopolymer” and also used several trademarks such as Pyrament, Geopolycem and Geopolymite for the binder (Davidovits 2002; Davidovits 1994). This type of materials virtually belongs to the alkaline binding system $Me_2O–Me_2O_3–SiO_2–H_2O$, as discovered by Glukhovsky in 1957 (Shi et al., 2006). Early researches have shown that geopolymers are cheap to produce and can be made when naturally occurring materials are mixed with NaOH and water (Davidovits, 1988; Smith and Comrie, 1988). Geopolymeric products do not have fixed stoichiometric composition due to presence of amorphous to semi-crystalline structure and crystalline Al–Si particles (Davidovits, 1991).

Much of the previous development of alkali-activated materials has been based on activated slags. But, there is significant potential for utilization of other by-products. An enormous amount of fly ash and other by product materials is generated from power plants and there is a constant need to find new uses for them. In the US, approximately 49% of the utility wastes are simply landfilled, 41% are contained in surface impoundments, and about 10% are disposed of by discharging into old quarry operations. Increasingly, the alkali-activated materials are stored “on site” due to reduced costs to the utilities (Shi et al., 2006).

The present study conducted on these alkali-activated materials is aimed at predicting their performance when used in the field, through nondestructive testing. For this purpose, ultrasonic pulse velocity method

was adopted. The pulse velocity method has been established as a reliable means of estimating properties and it provides reliable, quick, safe, inexpensive and non-invasive quality control of structural elements affected by earthquake, fatigue, conflagration or other catastrophic scenarios (Leslie & Cheeseman, 1949; Elvery, 1973; Bungey, 1982). The velocity of ultrasonic pulses traveling in a solid depends on the density and elastic properties of the material. Hence, ultrasonic pulse velocity can often be used to assess the overall quality of a material, as well as to determine their elastic properties (Marfisi et al., 2005). The testing technique involves the generation of pulses of longitudinal, elastic stress waves by an electro-acoustical transducer in direct contact with the surface of the concrete specimen being tested (Komlos et al., 1996). After traversing through the material, the pulses are received and converted into electrical energy by a second transducer. The velocity, *v*, is calculated from the distance, *l*, between the two transducers and the electronically measured transit time, *t*, of the pulse as:

$$v=l/t \quad (1)$$

Ultrasonic pulse velocity method is usually very helpful in detecting the presence of cracks in a structural element. The pulses are not transmitted through large air voids in a material. Hence if a void lies directly in the pulse path, the instrument will indicate the time taken by the pulse that circumvents the void by the quickest route. It is thus possible to detect large voids when a grid of pulse velocity measurements is made over a region in which these voids are located. A viscous material, such as a jelly or grease, is commonly used as a coupling agent to ensure that the vibrational energy enters the test object and can be detected by the receiving transducer (PUNDIT, 1992). A number of researchers have developed theoretical models for the prediction of relationships between pulse velocity and physico-mechanical properties, such as modulus of elasticity, compressive strength, density, porosity, and permeability (Panzera et al. 2011).

The primary goal of the paper is to determine the regression equations of the experimentally obtained compressive strength and modulus of elasticity values as functions of the experimental ultrasonic pulse velocity values for the alkali-activated materials. These regression equations can be used to predict the compressive strength and modulus of elasticity using the ultrasonic pulse velocities as input. In addition, the behavior of specimens subjected to gradually increasing compressive stress was observed. Equations were generated to establish the relationship between the applied compressive stress and the corresponding ultrasonic velocities. Subsequently, in order to predict the condition of a structural element under applied stress, the present study computes the extent of loading, or what fraction of the compressive load has already been exerted on the structure,

i.e., the ratio of the applied stress to the compressive strength. Equations were then generated to express this ratio as a function of the ultrasonic pulse velocities. In order to conduct the formulation, the 'R' statistical package was used for regression analysis.

2. Materials and Testing Methods

2.1 Materials

Class F fly ash used in this study conforming to ASTM C618 (Standard Specification for Coal Fly Ash and Raw or Calcined Natural Pozzolan for Use in Concrete), was obtained from a local coal power plant. The specific gravity, specific surface area and oxide composition are listed in Table 1. Ground granulated blast furnace slag or slag conforming to Grade 100 of ASTM C989 (Standard Specification for Slag Cement for Use in Concrete and Mortars) obtained from local steel plant were used in this study (Table 1).

The coarse aggregate used was 12.5 mm (½ in.) graded and crushed limestone conforming to ASTM C33/C33M – 13 (Standard Specification for Concrete Aggregates). The saturated surface dry (SSD) bulk specific gravity was 2.68. Locally available 4.75 mm (0.187 in.) graded river sand conforming to ASTM C33 was used for this study. The fineness modulus and the SSD bulk specific gravity of sand were 2.79 and 2.59, respectively. A commercially available high-range water reducing admixture (HRWRA), conforming to ASTM C494 Type F (Specification for Chemical Admixtures for Concrete), was used in this study.

Table 1 Properties of the Materials Used

Materials	Slag [a]	Fly Ash
Specific gravity	2.88	2.47
Specific surface(m^2/kg)	580 (Blaine)	490 (Blaine)
Loss on ignition, %	0.06	3.00
SiO_2, %	36.0	49.34
Al_2O_3, %	12.0	22.73
CaO, %	42.0	3.09
MgO, %	6.0	1.06
SO_3, %	0.2	0.97
$Na_2O + 0.685\ K_2O$, %	0.74	2.75
Fe_2O_3, %	1.8	16.01
Others, %	1.2	1.05

[a]The pH value (in water) for the slag is in the range of 10.5 ~ 12.7.

Table 2 shows the preliminary scheme for selection of precursor combinations. Based on the preliminary test results, which are described later, the mix proportions, as shown in Table 3, were selected in order to

compare their influences on the microstructural properties of the cementitious systems for different combinations of fly ash with slag replacement, at different ages and different temperatures. A total of 10 mixes are produced at each of the three different temperatures – 23˚C, 40˚C and 60˚C, using different combinations of fly ash, and slag. Thus a total of 30 different mixture proportions were used for the present study.

2.2 Mix Proportions

As the precursors are primarily composed of industrial by-products, they will lead to significant uncertainties in the characteristics of the finished product. Moreover, the activating solution reacts with the precursor through a polymerization mechanism, whose chemistry is yet to be fully decoded. This polymerization process governs the development of strength of the building material and it is dependent on several factors – (i) the ratio of SiO_2/Na_2O in the activating silicate solution; (ii) the ratio of SiO_2/Na_2O in the precursor-activating solution mixture (also known as Ms ratio or Ms modulus); (iii) the ratio of SiO_2/Al_2O_3 in the precursor; (iv) the ratio of water-to-geopolymer (or alkali activated binder) solids (w/s); and (v) the curing temperature, i.e., the temperature at which the polymerization is allowed to occur. Evidently, there are plenty of parameters which can be varied in order to study the change in behavior of the finished AAM concrete products. For the purpose of the present work, the mixture proportions were designed in such a way that an optimum Ms modulus can be selected from a range of possible values in the initial step. Later on, keeping this optimum Ms modulus fixed, the curing temperature and the proportion of different industrial by-products in the precursor were varied to conduct in-depth analyses on the behavior of the finished product. A suitable value for w/s, which ensured sufficient workability, was also kept fixed for all the mixture proportions to maintain uniformity. The rationale behind selection of each parameter was based on the suggestions and observations made by previous researchers.

Prominent researchers in the field of AAM concrete have shown that an alkali activated binder mix attains the highest compressive strength when the silicon to aluminum molar ratio (Si:Al) lies within the range of 1:1 and 3:1 (Davidovits, 1988). So, in the initial step, fly ash and sodium silicate solution (SiO_2/Na_2O = 2:1) were batched so that Si:Al ratio approximately equal to 2:1 would be maintained upon blending them.

The choice of Ms modulus was based on the findings and guidelines provided by previous researchers. Some of the researchers used Ms modulus of 2 (Hardjito et. al., 2002a; Hardjito et. al., 2003, 2004, 2005a, 2005b; Rangan et. al., 2005a, 2005b; and Hardjito and Rangan, 2005), while Skvara et al. (2006) in Czech Republic used a range of Ms modulus from 1.0 to 1.6. In order to achieve the optimum Ms modulus for the present study, a batch of

trial mixtures were prepared and tested for compressive strength of hardened geopolymer paste specimens. The different values of the Ms modulus used for the trial mixtures were 1.2, 1.4, 1.6, and 1.8. The Ms modulus of 1.4, which resulted in the best compressive strength was taken as the Ms modulus for all further mixture proportions to be used for the present study. The preliminary scheme for the selection of the desired precursor combinations are provided in Table 2.

The molarity of the NaOH solution used is another important factor affecting the compressive strength of the AAM concrete . Some researchers found that molarity in the range of 8 – 14 resulted in very high compressive strength values (Lloyd and Rangan 2010), whereas, maximum compressive strength was achieved at molarity of 12 by Mustafa Al Bakri et al. (2011). In the present study NaOH was used in the form of powder and not as a solution. So, the equivalent molarity of the NaOH in the present case was checked at the end of the mix design and it was computed to be 12.67. That value was in close agreement with the value suggested in the existing literature.

The temperature of curing is another aspect of the mixing procedure which deserves special attention. Previous research has already shown that if the starting materials are heated to a temperature in the range of 950°C (Han and Pyzik, 2011 and Pacheco-Torgal et al., 2007), then the finished geopolymer product exhibits excellent characteristics as a building material. However, a substantial amount of energy would be consumed in attaining such a high temperature. As mentioned previously, one of the main motivations behind the present research is to develop a sustainable construction material. So, the finished product must be economic as well as energy-efficient. From this point of view, the idea to heat the starting materials to elevated temperatures was rejected. Previous research by Rangan (2008) showed that, desirable compressive strength values were obtained if the curing temperature of 80˚C was used. Based on the findings from the research by Rangan (2008), three different curing temperatures of 23˚C (room temperature), 40˚C, and 60˚C were adopted for the present study. The idea is to compare the different properties of the finished product at different temperatures and propose an ideal curing temperature for practical uses of the material, which will optimize the economy and sustainability factors as well as the performance of the material for use in construction purposes.

As the present study makes a compromise on the temperature of curing, it was necessary to introduce Ca^{2+} ions into the system to enhance the compressive strength properties. This technique has been followed by a group of researchers in the past as well (Skvara et al., 2006). For the present study, slag was used as the source of Ca^{2+} ions. The Ca^{2+} ions impart

additional compressive strength by forming calcium silicate hydrate (C-S-H(S)) as a hydration product. Slag has weak hydraulic properties and the hydration of slag may be thought to be analogous to the hydration of Portland Cement (PC). The only difference is the formation of the secondary C-S-H which has different stoichiometry than the primary C-S-H produced by the hydration of PC. For the present study, different percentage replacements of fly ash by slag were adopted to identify the change in its mechanical and chemical characteristics. The different percentage replacements used in the present study are 15%, 30%, 50%, 70%, 85% and 100%. The 100% fly ash case is denoted as the datum or base case. The last three mixture proportions were studied in order to identify the effect of preblending the fly ash with the sodium hydroxide for varying durations of 15, 30 and 60 days. The preblending did not have any remarkable influence on the results of the present study.

The w/s was taken as 0.20 based on the calculations shown by Rangan (2008). This w/s worked satisfactorily for the 100% fly ash case. However, when slag was introduced into the system for partial replacement of fly ash, the workability was very poor and the mix became very stiff to cast into molds. So, high range water reducing admixture (HRWRA) was added accordingly in order to achieve desired workability. This was kept consistent for all mixture proportions used in the present study, and the mixture proportions encompassed all the above criteria.

Table 2 Preliminary Scheme for Selection of Precursor Combinations

Precursor	Alkali activating solution, AAS ($Na_2O.2SiO_2$ + NaOH)	Curing temps	Age (days)
100 % Fly ash	Total SiO_2 / Na_2O = 1.2, 1.4, 1.6, 1.8	23 °C, 40 °C, 60 °C	3, 7, 28

For initial assessment to estimate the best Ms ratio, the compressive strengths of 2 in. cube specimens were measured for different AAM mixtures as shown in Table 2 and Fig. 1. It was evident that Ms modulus of 1.4 resulted in the best compressive strengths at all ages and the strengths increased with curing temperature.

(a) (b)

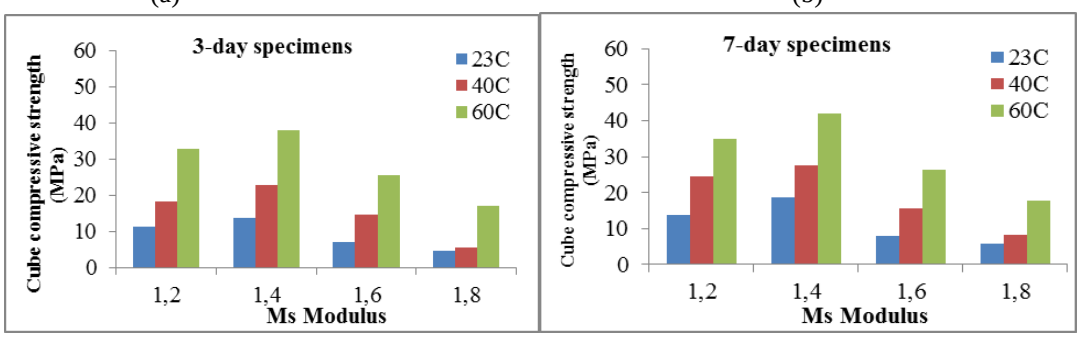

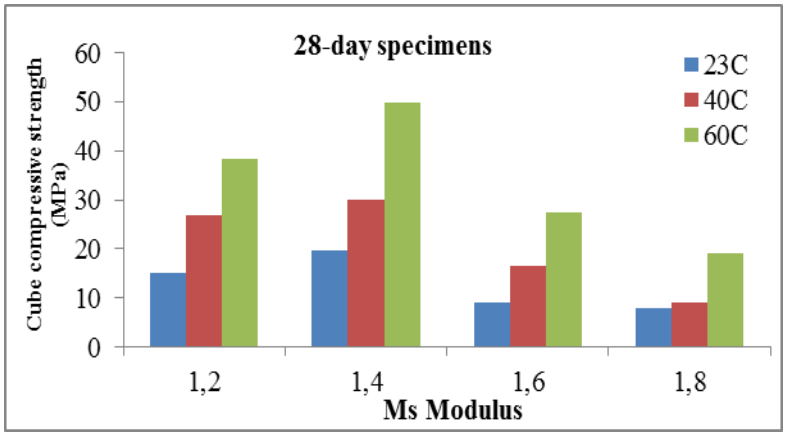

(c)

Fig. 1 Cube compressive strength for mixes from Table 2 at different Ms Modulus for specimens at different ages: (a) 3 days, (b) 7 days, and (c) 28 days.

Table 3 Final Concrete Mix Proportions for Alkali Activated Fly Ash and/or Slag

Precursor	Mixture Name	Fly ash	Slag	Sodium silicate (liquid)	Sodium hydroxide (solid)
		Kg/m^3	Kg/ m^3	Kg/m^3	Kg/ m^3
100 % Fly ash	FA 100	400	0	129.43	10.57
85% Fly ash + 15% slag	85/15	340	60	129.43	10.57
70% Fly ash + 30% slag	70/30	280	120	129.43	10.57
50% Fly ash + 50% slag	50/50	200	200	129.43	10.57
30% Fly ash + 70% slag	30/70	120	280	129.43	10.57
15% Fly ash + 85% slag	15/85	60	340	129.43	10.57
100% slag	SG 100	0	400	129.43	10.57
Pre blend 100% fly ash and solid NaOH for 15 days	FA 100 p15	400	0	129.43	10.57
Pre blend 100% fly ash and solid NaOH for 30 days	FA 100 p30	400	0	129.43	10.57
Pre blend 100% fly ash and solid NaOH for 60 days	FA 100 p60	400	0	129.43	10.57

Note: The quantity of coarse aggregate was kept constant at 1209 kg/m^3 and that of fine aggregate at 651 kg/m^3 for all mixes. The quantity of HRWRA used was in the range of 5060 ~ 6745 ml/m^3. The Ms modulus was 1.4 for all mixes.

The details of the experimental methods and the relevant models are discussed in the next section.

3. Experimental Methods

3.1 Ultrasonic Pulse Velocity Measurements

The ultrasonic pulse velocity test has been long established as an efficient nondestructive test method to determine the velocity of longitudinal (compressional) waves. As mentioned earlier, this determination consists of measuring the time taken by a pulse – leading to the name of the technique – to travel a measured distance. The apparatus includes transducers which are kept in contact with concrete, a pulse generator with a frequency in the range of 10 to 150 kHz, an amplifier, a time measuring circuit, and a digital display of the time taken by the pulse of longitudinal waves to travel between the transducers through the concrete. The test method follows the guidelines prescribed by ASTM C597-09 (C597-09 Standard Test Method for Pulse Velocity Through Concrete). The ultrasonic pulse velocities were obtained from tests on 75 mm × 75 mm × 275 mm (width × depth × length) prisms.

3.2 Dynamic Modulus of Elasticity

The dynamic modulus of elasticity values were measured on 101.6 mm diameter and 203.2 mm long cylinder specimens. The modulus of elasticity values were obtained in accordance with ASTM C215-08 (Standard Test Method for Fundamental Transverse, Longitudinal, and Torsional Resonant Frequencies of Concrete Specimens) on 7-day, 28-day, and 90-day old samples for each mixture proportion.

3.3 Compressive Strength Determination

Compressive strengths of 101.6 mm diameter and 203.2 mm long cylinder specimens were measured in accordance with ASTM C 39 (Standard Test Method for Compressive Strength of Cylindrical Concrete Specimens). Tests were conducted at 7, 28, and 90 days after casting. Both curing time and curing temperature influence the compressive strength of AAM concrete specimens. The specimens were cured after 24 hours of casting. Three different temperatures, i.e., 23˚C (room temperature) and 40˚C, and 60˚C (the last two temperatures were obtained in an oven) were used to cure the respective specimens for 24 hours. Average values of compressive strength of 3 specimens for each mixture proportion were used for the present study. Another set of experiments were conducted to study the behavior of AAM concrete to gradually increasing compressive stress using the cylindrical test specimens mentioned above. The observations were recorded for the corresponding ultrasonic pulse velocities at definite intervals of gradually increasing compressive loads to an extent that the loading was stopped just before the specimens failed in compression. For each of the specimens, 0.9 f_c' (i.e. the compressive strength for that particular mixture proportion) was chosen as the limit to which they were loaded. The results of the experiments and the pertinent observations for all the different experiments are furnished in the following section.

4. Results and Discussions

The results obtained from the different experiments are presented in this section and the data obtained from the experiments were used to make observations and conclusions about the characteristics of AAM concrete.

4.1 Compressive Strength Results for AAM Concrete Cylinders

The variation of compressive strength with age for all mixes at each curing temperature is shown in Fig. 2.

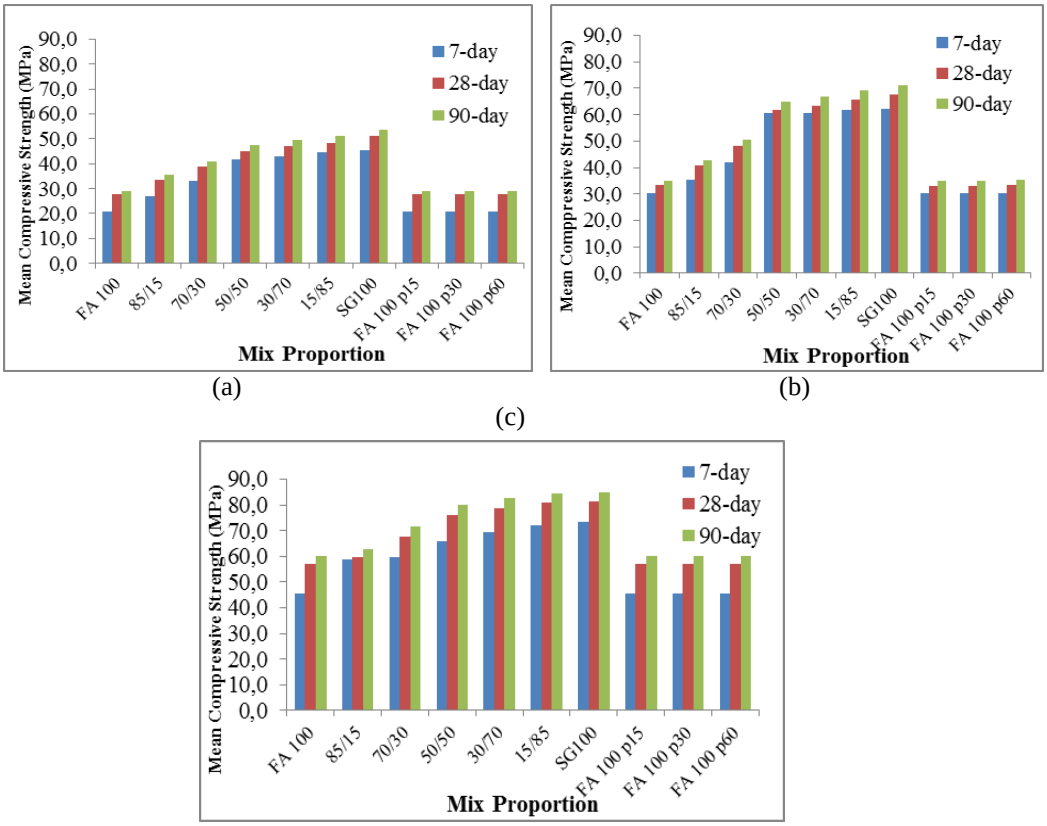

Fig. 2 Compressive strength data for all mixes at different ages at different temperatures: (a) 23˚C, (b) 40˚C, and (c) 60˚C

It was observed that the compressive strength increased with increase in percentage of slag in the precursor. The AAM concrete specimens made with fly ash as precursor had the least compressive strength while the AAM concrete specimens made with slag as precursor showed the highest compressive strength for all three temperature levels (Fig. 2). Preblending the fly ash with NaOH did not seem to have any influence on the compressive strength values. The increase of compressive strength with increasing curing temperature was observed for the AAM cubic specimens as well as the AAM concrete cylinders. The variations of dynamic modulus of

elasticity and compressive strength with ultrasonic pulse velocity have been shown in the following sections.

4.2 Variation of Dynamic Modulus of Elasticity with Ultrasonic Pulse

The wave velocity, *v*, in a homogeneous, isotropic and elastic medium is related to the dynamic modulus of elasticity, E_c, by the expression:

$$v^2 = \frac{E_c(1-\mu)}{\rho(1+\mu)(1-2\mu)} \quad (2)$$

Where ρ is density and μ is Poisson's ratio.

We can rewrite the eqn. (2) as

$$v^2 \propto E_c \quad (3)$$

Because density and Poisson's ratio are constants for a particular specimen and we typically assume that the different specimens corresponding to each mixture proportion possess more or less uniform density and Poisson's ratio characteristics. Normal concrete does not fulfill the physical requirements for the validity of the above expression and the determination of the modulus of elasticity of concrete from the pulse velocity is not generally advised. However, Nilsen and Aitcin (1992) showed the usefulness of this technique in case of high strength concrete in service. Although the value of the Poisson's ratio cannot always be determined with absolute accuracy, it varies within a small range of 0.16 to 0.25. The corresponding reduction in the computed value of the modulus of elasticity is only about 11%. So, the above technique can satisfactorily be used for field applications to estimate the modulus of elasticity from pulse velocity. The experimental results for modulus of elasticity and the corresponding ultrasonic pulse velocity results are provided in the next section. The developments of the relevant equations are also explained in detail.

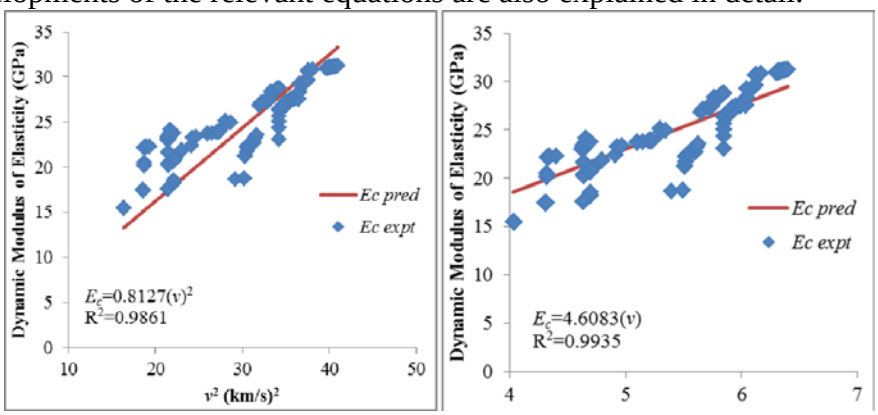

(a) (b)

Fig. 3(a) Variation of E_c vs. v^2 for all specimens and (b) Variation of E_c vs. *v* for all specimens

The results showed that the ultrasonic pulse velocity increased with increasing modulus of elasticity. In general, higher values of modulus of elasticity were obtained at higher temperatures. Linear regression was carried out using statistical software 'R'. Equations were obtained for the variation of modulus of elasticity, E_c, with the square of the ultrasonic pulse velocities, v^2 in accordance with eqn. (3). Equations were also obtained to express linear relationships between E and v. This provided a simpler form of the model. These relationships were obtained for each of the three curing temperatures. Another set of equations were generated for all the mixture proportions taken together, irrespective of the curing temperatures. For the sake of brevity, only the overall plots for variations of E_c vs. v^2 and E_c vs. v have been provided (Figs. 3(a) and (b)). The different equations for the cases mentioned above have been provided in the Table 4, along with their corresponding R^2 values.

Table 4 Variation of E_c vs. v^2 and E_c vs. v

Temperature	Equation	R^2
23˚C	$E_c = 0.7390v^2$	0.9824
	$E_c = 4.0849v$	0.9987
40˚C	$E_c = 0.8864v^2$	0.9923
	$E_c = 4.8227v$	0.9993
60˚C	$E_c = 0.8143v^2$	0.9944
	$E_c = 4.8630v$	0.9996
All specimens	$E_c = 0.8127v^2$	0.9861
	$E_c = 4.6083v$	0.9935

In order to understand the effects of the different curing temperatures, different equations were developed for each curing temperature. However, if the curing temperature is unknown during field applications, then the user can utilize the general equation obtained for all specimens taken together. For each of the cases, it was noticed that the equations obtained in case of E_c expressed as $f(v)$ showed slightly better R^2 values than the corresponding equations which expressed E_c as $f(v^2)$. At the same time, the linear model provides a simpler model for field use.

Thus, two different sets of equations were obtained in order to express the relationship between the modulus of elasticity values and the ultrasonic pulse velocities, for each of the three different curing temperatures, as well as for all the specimens considered together. The last set of equations would be useful if the curing temperature is unknown. In the field, it might be useful for the engineer to measure the ultrasonic pulse velocity at different locations on a structural element made out of AAM concrete. The suggested equations can then be used to predict the modulus of elasticity at the corresponding locations. These values can be used to detect the presence of deterioration in the structure. The modulus of elasticity

values increase with increasing ultrasonic pulse velocities. Hence, the presence of low values of the pulse velocity at any location in the structure, compared to its neighboring locations, will indicate low modulus of elasticity at that location. This will indicate the presence of deterioration to the field engineer. The relationship between the compressive strength and the ultrasonic pulse velocity is discussed in details in the following section.

4.3 Variation of Compressive Strength with Ultrasonic Pulse Velocity

It has been established by researchers that the modulus of elasticity of concrete increases with its compressive strength, but there are different theories on the exact relationship between these two parameters. The expression for the modulus of elasticity of concrete, E_c, in psi units, recommended by ACI 318-11: Building Code Requirements for Structural Concrete and Commentary, for structural calculations, applicable to normal weight concrete, is

$$E_c = 57000\sqrt{f'_c} \quad (4)$$

Where f'_c is the compressive strength of standard test cylinders in psi units.

The above expression can be rewritten as

$$f'_c \propto E_c^2 \quad (5)$$

Combining eqns (3) and (5), we can write

$$f'_c \propto v^4 \quad (6)$$

The present study aims at establishing an equation to correlate the compressive strength and the ultrasonic pulse velocity. In the field, if the ultrasonic pulse velocity is measured at different locations in a structure, the compressive strength values can be predicted. Thus, the load carrying capacity of the structure can be estimated. Moreover, if the estimated values show some anomalies at certain locations, the possibility of deterioration due to cracks can be determined.

The relationship between the modulus of elasticity and the compressive strength as mentioned earlier, holds good for portland cement concrete. As the present study deals with a different material, it is necessary to establish a different set of equations to describe the relationship between the modulus of elasticity and the compressive strength for this new material. The parameter that is measured in the field is the ultrasonic pulse velocity. The present study develops equations to express the modulus of elasticity as a function of the ultrasonic pulse velocity and also the compressive strength as a function of the ultrasonic pulse velocity.

Theoretically, the modulus of elasticity is proportional to the square of the ultrasonic pulse velocity and the compressive strength is proportional to the fourth power of the ultrasonic pulse velocity. Hence the present study

expresses $E_c = f(v^2)$ and $f_c' = f(v^4)$. However, if the predicted values of E_c or f_c' (determined by expressing them as functions of v) lies in the linear region of their respective curves (i.e., away from the origin), then E_c or f_c' can both be linearly correlated with v. Therefore, the present study expresses $E_c = f(v)$ and $f_c' = f(v)$ in addition to the aforementioned second and fourth power expressions. Different graphs were obtained for the three different temperatures used in the study. The curing depends on the temperature. In the field, a curing temperature of 40˚C can be achieved throughout the day and night in some places like the Indian subcontinent, mid-western Africa, Northern and North Eastern parts of South America and some islands in the Indian Ocean, which have tropical climate. On the other hand, 60˚C temperature can be achieved only with the use of an oven, which is mainly suitable for precast units. From the compressive strength test results, it was observed that the gain in compressive strength due to curing at 60˚C is 19.38% compared to those cured at 40˚C. But curing at higher temperature involves high amount of energy consumption. So, it might be advisable, especially in the case of developing and under-developed countries, to compromise on the compressive strength to some extent and adopt a curing temperature of 40˚C. This approach is encouraged based on sustainability criteria. In this study, relationships were developed for each of the curing temperatures, and also for the combined set of the compressive strength data for all the specimens taken together irrespective of the curing temperature. This is of great use in predicting the compressive strength from the ultrasonic pulse velocity value when the curing temperature is unknown.

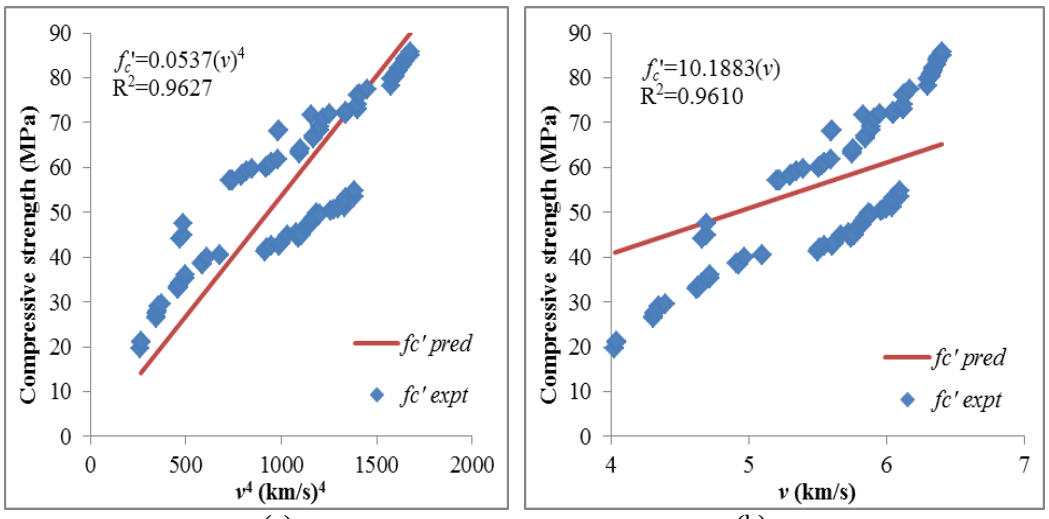

(a) (b)

Fig. 4(a) Variation of f_c' vs. v^4 for all specimens and (b) Variation of f_c' vs. v for all specimens

The results showed that the ultrasonic pulse velocities increased with increasing compressive strength. In general, higher values of compressive strength were obtained at higher temperatures. The highest compressive strength was obtained for the 90-day age specimens cured at 60˚C for 24 hours. Linear regression was carried out using 'R' statistical package. Equations were obtained for the variation of compressive strength, f_c', with the fourth power of the ultrasonic pulse velocities, v^4, as well as between f_c' and v. The latter case was considered in order to obtain a simpler model. These relationships were obtained for each of the three curing temperatures. Another set of equations were generated for all the mixture proportions taken together, irrespective of the curing temperatures. For the sake of brevity, only the overall plots for variation of f_c' vs. v^4 and f_c' vs. v have been provided (Figs. 4 (a) and (b)). The different equations for the cases mentioned above have been provided in Table 5, along with their corresponding R^2 values.

Table 5 Variation of f_c' vs. v^4 and f_c' vs. v

Temperature	Equation	R^2
23˚C	$f_c' = 0.04385v^4$	0.9576
	$f_c' = 7.78494v$	0.9904
40˚C	$f_c = 0.06178v^4$	0.9764
	$f_c' = 10.3708v$	0.9808
60˚C	$f_c' = 0.05501v^4$	0.9833
	$f_c' = 12.009v$	0.9943
All specimens	$f_c' = 0.0537v^4$	0.9627
	$f_c' = 10.1883v$	0.9610

As in the case of modulus of elasticity, different equations were developed for each curing temperature in order to understand the effects of the different curing temperatures. However, if the curing temperature is unknown during field applications, then the user can utilize the general equation obtained for all specimens taken together. For each of the cases, it was noticed that the equations obtained in case of f_c' expressed as $f(v)$ showed slightly better R^2 values than the corresponding equations which expressed f_c' as $f(v^4)$.

Thus, two different sets of equations were obtained in order to express the relationship between the modulus of elasticity values and the ultrasonic pulse velocities, for each of the three different curing temperatures, as well as for all the specimens considered together. The last set of equations would be useful if the curing temperature is unknown. In the field, it might be useful for the engineer to measure the ultrasonic pulse velocity at different locations on a structural element made out of AAM concrete. The suggested equations can then be used to predict compressive strength at the corresponding locations. These values can be used to detect

the presence of deterioration in the structure if some locations show low ultrasonic pulse velocities which will imply loss of compressive strength, and hence, the presence of deterioration.

In case of field evaluation or in-situ testing of structures to be built out of AAM, it is necessary to have an estimate of the load carrying capacity of a structure and the detection of cracking in a structure. Based on the ultrasonic pulse velocity results, the user will have an idea about the extent to which the structure has been loaded or the extent of failure of the structure. The velocities will be measured at different locations on the structure and the user will be looking for anomalies in the results. If the velocities are very low at some locations as compared to the others, it means that the structure has been loaded to a great extent at those particular points and there is possibility of high amount of cracking and potential failure. For this purpose, the present study also investigated the variation of the ultrasonic pulse velocity with gradually increasing compressive loading (up to 90% of the measured compressive strength determined previously) on standard test cylinders made out of the material used in the study. Relationships were developed to express the applied stress as linear functions of v as well as v^4. The relevant plots and results are discussed in details in the following section.

4.4 Variation of Gradually Increasing Applied Compressive Stress with Ultrasonic Pulse Velocity

In order to determine the effect of compressive stress that has been exerted on the structure, the present study investigated the variation of ultrasonic pulse velocity with applied compressive stress (σ_c) on AAM concrete specimens. The specimens used for this experiment were same as the cylinders used for dynamic modulus of elasticity and compressive strength determination. Plots were made and equations were developed at each temperature to express σ_c as functions of v and v^4. These experiments were conducted on 28-day old specimens only.

The results showed that the maximum ultrasonic pulse velocities were observed at zero applied stresses. In other words, the ultrasonic pulse velocities were the largest when the concrete specimen was not subjected to any stress, i.e., there was no deterioration. As the applied stress was increased gradually, the ultrasonic pulse velocities decreased appreciably. The lowest ultrasonic pulse velocities were observed when the applied stresses were the largest, i.e., when the concrete specimen was close to failure. Linear regression was carried out using 'R' statistical package. Equations were obtained for the variation of applied strength, σ_c, with the fourth power of the ultrasonic pulse velocities, v^4, as well as between σ_c and v. These relationships were obtained for each of the three curing temperatures. Another set of equations were generated for all the mixture

proportions taken together, irrespective of the curing temperatures. For the sake of brevity, only the overall plots for variation of σ_c vs. v^4 and σ_c vs. v have been provided (Figs. 5(a) and (b)). The different equations for the cases mentioned above have been provided in Table 6, along with their corresponding R^2 values. For each of the cases, it was noticed that the equations obtained in case of σ_c expressed as $f(v)$ showed better R^2 values than the corresponding equations which expressed σ_c as $f(v^4)$.

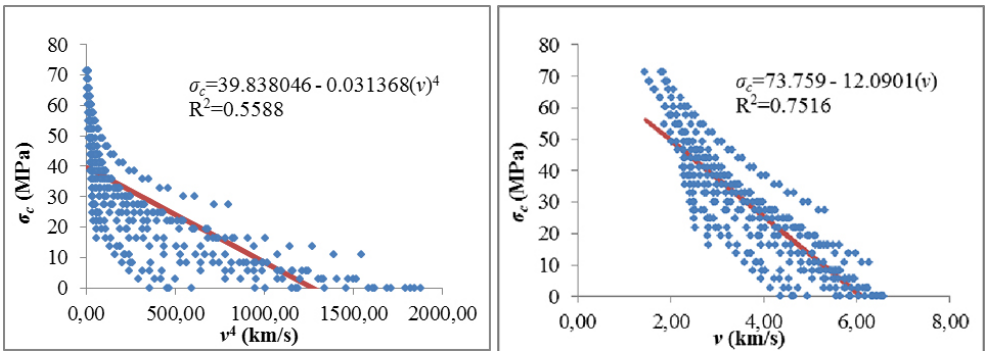

(a) (b)

Fig. 5(a) Variation of σ_c vs. v^4 for all specimens and (b) Variation of σ_c vs. v for all specimens at 28 days

Table 6 Variation of σ_c vs. v^4 and σ_c vs. v

Temperature	Equation	R^2
23˚C	$\sigma_c = 28.5419-.0282v^4$	0.5438
	$\sigma_c = 55.5818-9.807v$	0.7470
40˚C	$\sigma_c = 38.9706-0.0311v^4$	0.6125
	$\sigma_c = 74.7488-12.1963v$	0.7777
60˚C	$\sigma_c = 47.5657-0.0349v^4$	0.7182
	$\sigma_c = 83.1580-13.2371v$	0.9187
All specimens	$\sigma_c = 39.8380-0.0314v^4$	0.5588
	$\sigma_c = 73.7590-12.0901v$	0.7516

Subsequently, in order to find out the extent of loading, or what fraction of the compressive load has already been exerted on the structure, the present study looked at the ratio of the applied stress to the compressive strength ratio (σ_c/f_c') of concrete specimens. Plots were made and equations were developed at each temperature to express σ_c/f_c' as functions of v and v^4. These experiments were conducted on 28-day old specimens only.

The results showed that the maximum ultrasonic pulse velocities were observed when the σ_c/f_c' ratio was zero, i.e., at zero applied stresses. In other words, the ultrasonic pulse velocities were the largest when the concrete specimens were not subjected to any stress, i.e., there was no deterioration. As the σ_c/f_c' ratio was increased gradually, the ultrasonic pulse velocities decreased appreciably. The lowest ultrasonic pulse velocities were

observed when the σ_c/f_c' ratios were the largest, i.e., when the concrete specimen was close to failure. Linear regression was carried out using 'R' statistical package. Equations were obtained for the variation of σ_c/f_c' ratio with the fourth power of the ultrasonic pulse velocities, v^4, as well as between σ_c/f_c' ratio and v. These relationships were obtained for each of the three curing temperatures. Another set of equations were generated for all the mixture proportions taken together, irrespective of the curing temperatures. For the sake of brevity, only the overall plots for variation of σ_c/f_c' ratio vs. v^4 and σ_c/f_c' ratio vs. v have been provided (Figs. 6(a) and (b)). The different equations for the cases mentioned above have been provided in Table 7, along with their corresponding R^2 values. For each of the cases, it was noticed that the equations obtained in case of σ_c/f_c' ratio expressed as $f(v)$ showed better R^2 values than the corresponding equations which expressed σ_c/f_c' ratio as $f(v^4)$.

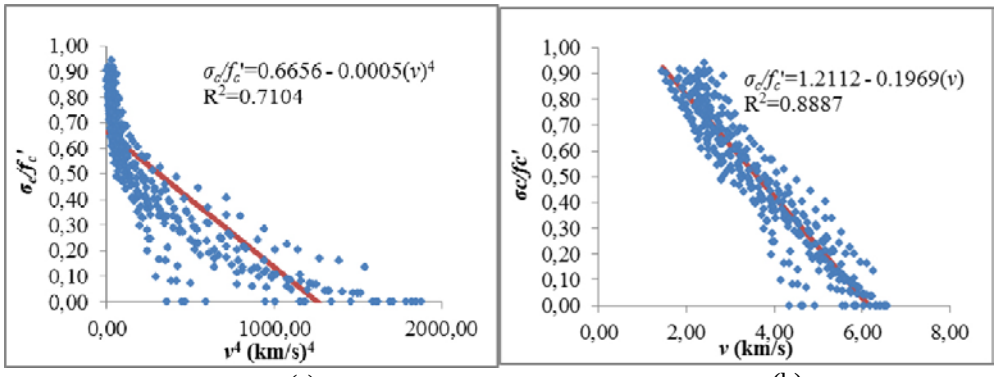

(a) (b)

Fig. 6(a) Variation of σ_c/f_c' vs. v^4 for all specimens and (b) Variation of σ_c/f_c' vs. v for all specimens at 28 days

Table 7 Variation of σ_c/f_c' vs. v^4 and σ_c/f_c' vs. v

Temperature	Equation	R^2
23˚C	$\sigma_c/f_c' = 0.6694-0.0007v^4$	0.6437
	$\sigma_c/f_c' = 1.2833-0.2263v$	0.8370
40˚C	$\sigma_c/f_c' = 0.6944-0.0006v^4$	0.7417
	$\sigma_c/f_c' = 1.3238-0.2161v$	0.9034
60˚C	$\sigma_c/f_c' = 0.6545-0.0005v^4$	0.7703
	$\sigma_c/f_c' = 1.1356-0.1798v$	0.9572
All specimens	$\sigma_c/f_c' = 0.6657-0.0005v^4$	0.7104
	$\sigma_c/f_c' = 1.2112-0.1969v$	0. 8887

5. Conclusions

Based on the above studies the following conclusions are made:

1. It was observed that the compressive strength increased with the increasing percentage of slag added to AAM concrete for all curing

conditions and ages. This highlights the beneficial effects of slag as calcium ions to enhance the strength of only aluminosilicate (fly ash) precursor.

2. The ultrasonic pulse velocity increased with increasing dynamic modulus of elasticity. The modulus of elasticity was proportional to the square of the ultrasonic pulse velocity with significantly high R^2 values. This was true for each of the curing temperatures studied.

3. The relationships between modulus of elasticity and ultrasonic pulse velocity was found to follow the same trend for different curing temperatures enabling the technique to be used in case of AAM concrete having unknown curing temperature.

4. The compressive strength was found to be proportional to the fourth power of ultrasonic pulse velocity, but the linear correlation between compressive strength and ultrasonic velocity also produced good results. This was true for each of the curing temperatures as well as for the combined data set of all the curing temperatures. This makes it possible to use the ultrasonic technique for predicting strength of AAM concrete having unknown curing temperature.

5. The ultrasonic pulse velocities were found to be largest when the AAM concrete specimens were not subjected to any stress, i.e., there was no deterioration. As the σ_c/f_c' ratio was increased gradually, the ultrasonic pulse velocities decreased appreciably. The lowest ultrasonic pulse velocities were observed when the σ_c/f_c' ratios were the largest, i.e., when the concrete specimen was close to failure.

6. By normalizing the stress level (σ_c) of different AAM concrete with respect to their corresponding ultimate strengths (f_c'), a linear relationship was found to exist between the σ_c/f_c' ratio and the ultrasonic pulse velocity.

7. This paper has shown that the ultrasonic pulse velocity technique can be effectively used to estimate the modulus of elasticity, compressive strength, and stress level of AAM concrete for wide range of mixes, curing temperature, and ages. This will help in monitoring the quality control and deterioration of the different AAM concrete structures in the field. Even in case of existing AAM concrete structures where curing temperature, ages, and AAM mix sources are not known, the present correlations can still be used to estimate the strength, modulus of elasticity, and stress level with reasonable accuracy.

Acknowledgements:

Special thanks are due to the American Society of Civil Engineers (ASCE) for providing the 2012 ASCE Freeman Fellowship to the first author in support of this research. The authors gratefully acknowledge Arrow concrete for donating fly ash and slag, and PQ Corporation for providing the sodium silicate solution used in the present study. The authors would also

like to acknowledge Sriparna Ghosh, graduate student at West Virginia University, for her help with some of the laboratory works.

References:

ASTM C33M-13 (Standard Specification for Concrete Aggregates), Annual Book of ASTM Standards, Vol. 04.02, Concrete and Aggregates, American Society for Testing and Materials, 2013.
ASTM C39/C39M-12a (Standard Test Method for Compressive Strength of Cylindrical Concrete Specimens), Annual Book of ASTM Standards, Vol. 04.02, Concrete and Aggregates, American Society for Testing and Materials, 2013.
ASTM C215-08 (Standard Test Method for Fundamental Transverse, Longitudinal, and Torsional Resonant Frequencies of Concrete Specimens), Annual Book of ASTM Standards, Vol. 04.02, Concrete and Aggregates, American Society for Testing and Materials, 2013.
ASTM C494 Type F (Specification for Chemical Admixtures for Concrete), Annual Book of ASTM Standards, Vol. 04.02, Concrete and Aggregates, American Society for Testing and Materials, 2013.
ASTM C597-09 (C597-09 Standard Test Method for Pulse Velocity Through Concrete), Annual Book of ASTM Standards, Vol. 04.02, Concrete and Aggregates, American Society for Testing and Materials, 2013.
ASTM C618 (Standard Specification for Coal Fly Ash and Raw or Calcined Natural Pozzolan for Use in Concrete), Annual Book of ASTM Standards, Vol. 04.02, Concrete and Aggregates, American Society for Testing and Materials, 2013.
ASTM C989 (Standard Specification for Slag Cement for Use in Concrete and Mortars), Annual Book of ASTM Standards, Vol. 04.02, Concrete and Aggregates, American Society for Testing and Materials, 2013.
British Standard BS EN 12504-4, Testing concrete, Determination of ultrasonic pulse velocity, 2004.
Bungey J. H., The Testing of Concrete in Structures, SUNY University Press, New York,1982.
Davidovits, J., "Geopolymers of the First Generation: SILIFACEProcess". In: Davidovits, J., Orlinski, J. (Eds.), Proceedings of the 1st International Conference on Geopolymer '88, Vol. 1, Compiegne, France, 1–3 June, pp. 49–67 pp., 1988.
Davidovits, J. "Geopolymers: Inorganic polymeric new materials", Journal of Thermal Analysis, Vol. 37, pp. 1633–1656 pp., 1991.
Davidovits, J., "Geopolymers: Inorganic polymeric new materials", Journal of Materials Education, Vol. 16, pp. 91–139 pp., 1994.

Davidovits, J., "30 Years of Successes and Failures in Geopolymer Applications. Market Trends and Potential Breakthroughs.", Geopolymer 2002 Conference, October 28-29, 2002, Melbourne, Australia, 2002

Elvery R. H., "Estimating strength of concrete in structures", Current Practice Sheet 10, Concrete, Vol. 11, No. 7, 49–51 pp., 1973.

Han, C. and Pyzik, A. J., "Geopolymer precursor dry mixture, package, processes and methods", United States Patent Application Publication, Pub No. US 2011/0132230 A1, June 2011.

Hardjito, D. and Rangan, B.V., "Development and properties of low-calcium fly ash-based geopolymer concrete", Research Report GC 1, Faculty of Engineering, Curtin University of Technology, Perth, Australia, 2005.

Hardjito, D., Wallah, S. E., & Rangan, B. V., "Research Into Engineering Properties of Geopolymer Concrete", Paper presented at the Geopolymer 2002 International Conference, Melbourne, 2002a.

Hardjito, D., Wallah, S. E., & Rangan, B. V., "Study on Engineering Properties of Fly Ash-Based Geopolymer Concrete", Journal of the Australasian Ceramic Society, Vol. 38, No. 1, 44-47 pp., 2002b.

Hardjito, D., Wallah, S. E., Sumajouw, D. M. J., & Rangan, B. V., "Geopolymer Concrete: Turn Waste Into Environmentally Friendly Concrete", Paper presented at the International Conference on Recent Trends in Concrete Technology and Structures (INCONTEST), Coimbatore, India, 2003.

Hardjito, D., Wallah, S. E., Sumajouw, D. M. J., & Rangan, B. V., "On the Development of Fly Ash-Based Geopolymer Concrete", ACI Materials Journal, Vol. 101, No. 6, 467 – 472 pp., 2004.

Hardjito, D., Wallah, S. E., Sumajouw, D. M. J., & Rangan, B. V., "Fly Ash-Based Geopolymer Concrete", Australian Journal of Structural Engineering, Vol. 6, No. 1, 77 – 86 pp., 2005a.

Hardjito, D., Wallah, S. E., Sumajouw, D. M. J., & Rangan, B. V., "Introducing Fly Ash-Based Geopolymer Concrete: Manufacture and Engineering Properties", Paper presented at the Our World in Concrete and Structures International Conference, Singapore, 2005b.

Hardjito, D., Wallah, S.E., Rangan, B.V., "Research into engineering properties of geopolymer concrete", In: Lukey, G.C. (Ed.), Proceedings of the International Conferenceo on Geopolymers, Melbourne, Australia, 28–29 October (in CD-ROM) , 2002.

Komlos K., Popovics S., Niirnbergeroh T., Babd B. and Popovics J. S., "Ultrasonic Pulse Velocity Test of Concrete Properties as Specified in Various Standards", Cement and Concrete Composites, Vol. 18, 357-364 pp., 1996.

Leslie J. R. and Chessman W. J., "An ultrasonic method of studying deterioration and cracking in concrete structures", Journal of American Concrete Institute, Vol. 21, No. 1, 17-35 pp., 1949.
Lloyd, N. A. and Rangan, B. V., "Geopolymer Concrete with Fly Ash", Coventry University and The University of Wisconsin Milwaukee Centre for By-products Utilization Second International Conference on Sustainable Construction Materials and Technologies June 28 - June 30, 2010, Università Politecnica delle Marche (UNIVPM), Ancona, Italy, 2010
Marfisi E., Burgoyne C. J., Amin M. H. G. and Hall L. D., "The use of MRI to observe the structure of concrete", Magazine of Concrete Research, Vol. 57, No. 2, 101–109 pp., 2005.
Mustafa Al Bakri, A. M , Kamarudin, H., Bnhussain, M., Khairul Nizar, I., Rafiza, A. R., and Zarina, Y., "Microstructure of different NaOH molarity of fly ash-based green polymeric cement", Journal of Engineering and Technology Research Vol. 3, No. 2, 44-49 pp., 2011.
Nilsen, A. U. and Aitcin, P.-C., "Static modulus of elasticity of high-strength concrete from pulse velocity tests", Cement, Concrete and Aggregate, Vol. 14, No. 1, 64 – 66 pp., 1992.
Pacheco-Torgal , F., Castro-Gomes, J., and Jalali, S., "Investigations about the effect of aggregates on strength and microstructure of geopolymeric mine waste mud binders", Cement and Concrete Research, Vol. 37, 933–941 pp., 2007.
Panzera, T. H., Christoforo, A. L., Cota, F. P., Borges, P. H. R. and Bowen, C. R., "Ultrasonic Pulse Velocity Evaluation of Cementitious Materials", Advances in Composite Materials - Analysis of Natural and Man-Made Materials, Chapter 17, book edited by Pavla Těšinova, ISBN 978-953-307-449-8, Published: September 9, 2011 under CC BY-NC-SA 3.0 license, DOI: 10.5772/17167, 2011.
Provis, J. L. and van Deventer, J. S. J., Geopolymers: structure, processing, properties and industrial applications, Publisher: Oxford: Woodhead ; Boca Raton, FL : CRC Press, 2009.
PUNDIT manual for use with the portable ultrasonic non-destructive digital indicating tester, MARK V, C. N. S. Electronics LTD, London, 1992.
Rangan, B.V, "Low-Calcium, Fly-Ash-Based Geopolymer Concrete", Concrete Construction Engineering Handbook, Chapter 26, Edited by Nawy, E. G., CRC Press 2008, Print ISBN: 978-0-8493-7492-0, eBook ISBN: 978-1-4200-0765-7, DOI: 10.1201/9781420007657.ch26., 2008.
Rangan, B.V., Hardjito, D., Wallah, S.E., Sumajouw, D.M.J., "Studies on fly ash-based geopolymer concrete." In: Davidovits, J. (Ed.), Proceedings of the World Congress Geopolymer, Saint Quentin, France, 28 June – 1 July, 133–137 pp., 2005.

Shi, C., Krivenko, P., and Roy, M., "Alkali-Activated Cements and Concretes", Taylor & Francis, London and New York, 2006.
Skvara, F., Kopecky, L., Nemecek, J., and Bittnar, Z., "Microstructure of geopolymer materials based on fly ash", Cermaics – Silikaty, Vol. 50, 208 – 215 pp., 2006.
Smith, J.W., Comrie, D.C., Geopolymeric building materials in third world countries. In: Davidovits, J., Orlinski, J. (Eds.), *Proceedings of the 1st Int. Conf. Geopolymer '88*, Vol. 1, Compiegne, France, 89–92 pp., 1–3 June 1988.